Improving Worst-Case End-to-End Delay Analysis of Multiple Classes of AVB Traffic in TSN Networks using Network Calculus

Luxi Zhao, Paul Pop, Zhong Zheng, Hugo Daigmorte and Marc Boyer

December 20, 2018

***Abstract*—Time-Sensitive Networking (TSN) is a set of amendments that extend Ethernet to support distributed safety-critical and real-time applications in the industrial automation, aerospace and automotive areas. TSN integrates multiple traffic types, in which one solution is supporting Time-Triggered (TT) traffic scheduled based on Gate-Control-Lists (GCLs), Audio-Video-Bridging (AVB) traffic according to IEEE 802.1BA that has bounded latencies, and Best-Effort (BE) traffic, for which no guarantees are provided. This paper proposes an improved timing analysis method reducing the pessimism for the worst-case end-to-end delays of AVB traffic by considering the limitations from the physical link rate and the output of Credit-Based Shaper (CBS). Moreover, the paper extends the timing analysis method to multiple AVB classes and proofs the AVB credit bounds of CBS for multiple classes, which are prerequisites for non-overflow of CBS credits and preventing starvation of AVB traffic. Finally, we evaluate the improved analysis method on both synthetic and real-world test cases, showing the significant reduction of pessimism on latency bounds compared to related work, and the correctness validation compared with simulation results. Additionally, we evaluate the scalability of our implementation with variation of the load of TT flows and the number of AVB classes.**

I. Introduction

ETHERNET is a well-established network protocol that has excellent bandwidth, scalability, compatibility and cost properties [1]. However, it is not suitable for real-time and safety critical applications [2]. Distributed safety-critical applications, like those found in the aerospace, automotive and industrial automation domains, require certification evidence for the correct real-time behavior of critical communication. Therefore, several extensions to the Ethernet protocol have been proposed, such as, ARINC 664 Specification Part 7 [3], TTEthernet [4], and EtherCAT [5]. In 2012, the IEEE 802.1 Time-Sensitive Networking (TSN) Task Group [6] has been founded to define standard real-time and safety-critical enhancements for Ethernet.

In this paper we consider a TSN solution supporting Credit-Based Shaper (CBS) (previously defined for Audio-Video Bridging (AVB) in 802.1BA [7], currently in [6, § 8.6.8.2] with the 802.1Qbv [8] enhancements for Scheduled Traffic (now in [6, § 8.6.8.4]) that add a Gate-Control Lists (GCLs). We consider three traffic-types with varying the criticality: Time-Triggered (TT) traffic (high priority), AVB traffic (medium priority) and Best-Effort (BE) traffic (low priority). TT traffic supports hard real-time applications that require very low latency and jitter. It has the highest priority and is transmitted based on schedule tables called GCLs that rely on a global synchronized clock (802.1ASrev [9]). AVB traffic is intended for applications that require bounded end-to-end latencies, but has a lower priority than TT traffic. It uses the CBS to prevent the starvation of lower priority AVB traffic. The TSN Task Group has extended AVB architecture, allowing the definition of multiple CBS, so we consider any number of AVB classes. BE traffic is used for applications that do not require any timing guarantees and is mapped to the remaining low priority queues. We call this architecture TSN/GCL+CBS.

The schedulability of the scheduled TT traffic can be guaranteed during design phase, by synthesizing the GCLs [10]. However, an AVB flow is schedulable only if its worst-case end-to-end delay (WCD) is smaller than its deadline. Moreover, AVB in TSN is envisioned for time-critical applications that require bounded latency, hence it is very important to have a safe and guaranteed WCD analysis for AVB that takes into account the TT flows. Although latency analysis methods have been successfully applied to AVB traffic in AVB networks [11], [12], [13], [14], [15], they do not take account for the interference of TT traffic on the AVB traffic and only consider two or three AVB classes. A Network Calculus-based analyses to compute the WCDs of Rate-Constrained (RC) traffic with the consideration of the static scheduled TT frames in TTEthernet have been proposed [16], [17], [18], but the techniques are not applicable for TSN: RC traffic has no CBS, and TSN schedules TT traffic differently from TTEthernet: individual TT frames are considered in TTEthernet, whereas TSN schedules TT windows may including several TT frames.

The timing analysis of non-TT traffic classes in TSN has been addressed in [19], considering closed-gate blocking, strict priorities and a “Peristaltic Traffic Shaper”. However, their analysis is not applicable to AVB, which uses CBS. [20] gives the latency bounds for AVB traffic affected by control-data-traffic (CDT) in TSN, but assuming CDT as leaky bucket (LB) or length rate quotient (LRQ), which does not fit for

L.X. Zhao and P. Pop are with the Department of Applied Mathematics and Computer Science, Technical University of Denmark, Copenhagen, Denmark, e-mail: luxzha@dtu.dk; paupo@dtu.dk.

Z. Zheng is with the Department of Electronics and Information Engineering, Beihang University, Beijing, China, e-mail: zhengzhong@buaa.edu.cn

H. Daigmorte and M. Boyer are with the Department on ”Information Processing and Systems” at ONERA, Toulouse, France, e-mail: Hugo.Daigmorte@onera.fr; Marc.Boyer@onera.fr.

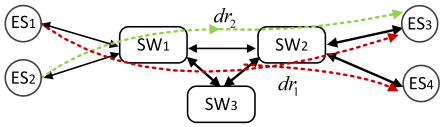

Fig. 1. TSN network topology example

the TT traffic. Researchers have extended the Eligible Interval analysis [14] to calculate the delay of AVB traffic in TSN [21]. However, it only focuses on the latency bounds through a single node and does not consider relative offsets between TT windows, but just assumes the TT windows always arranging back-to-back. The AVB Latency Math equation has been extended to consider the TT traffic in TSN [22]. However, it does not consider the actual situations for AVB flows in the network, but just assumes that maximum allocable bandwidth is occupied by the corresponding AVB traffic class, thus causing overly pessimistic, i.e., leading to overly large WCDs. In addition, [22] can only be used to determine the WCDs of AVB Class A traffic. The initial idea on the AVB analysis in TSN network based on the Network Calculus has been given by [23], but the WCDs results are pessimistic. Moreover, only two AVB traffic classes are in consideration in [23], but the latest standard 802.1Q-2018 [24] supports any number of AVB classes, and adding new classes requires additional proof for associated credit bounds[(1)].

The main contributions of our paper are as follows:

- We propose a Network Calculus-based method from [23] for the general case with arbitrary number of AVB traffic classes in a TSN network, which requires a proof of credit bounds of CBS for multiple AVB classes.
- We reduce the pessimism of the analysis and this provides tighter latency bounds for AVB, by introducing the limitations from the physical link rate and the output of CBS, which are denoted as the link and CBS shaping curves with the consideration of TT traffic.
- We evaluate the proposed approach on both synthetic and real-world test cases, and compare it with related work and simulation results to show the significant reduction of pessimism on latency bounds, and to validate the correctness and the scalability of our implementation.

The paper is organized as follows. Sect. II presents the architecture and application models. Sect. III introduces TSN. Sect. IV briefly introduces the Network Calculus concepts needed for the analysis. Sect. V gives the proof of credit bounds for multiple classes of AVB traffic and presents tighter AVB latency bounds by introducing shaping curves. Sect. VI evaluates the proposed analysis and Sect. VII concludes the paper.

II. System Model

A TSN network is composed of a set of end systems (ES) and switches (SW) also called nodes, connected via physical links. In this paper, we assume, without loss of generality, that all physical links have the same rate C. The links are

[(1)]Even going from 2 to 3 requires specific work [15].

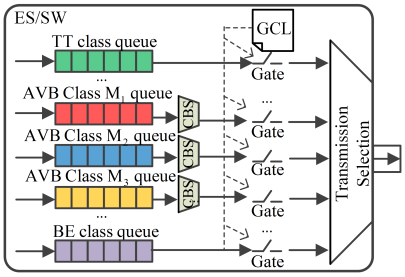

Fig. 2. TSN/GCL+CBS architecture for an output port in an ES/SW

full duplex, allowing thus communication in both directions, and the networks can be multi-hop. The output port of a SW is connected to one ES or an input port of another SW. An example is presented in Fig. 1, where we have 4 ESes, ES_1 to ES_4, and 3 SWs, SW_1 to SW_3. A dataflow routing $dr_i \in \mathbf{R}$ is statically defined as a directed ordered sequence of physical links connecting a single source ES to one or more destination ESes. For example, in Fig. 1, dr_1 connects the source end system ES_1 to the destination end systems ES_3 and ES_4, while dr_2 connects ES_2 to ES_3.

The messages running in the ESes communicate via flows, which have a single source and may have multiple destinations. Each source ES is able to send multiple flows to the network. As mentioned, TSN supports three traffic classes: TT, AVB and BE. We assume that the traffic class for each application has been decided by the designer and we define the sets τ_{TT}, τ_{M_i}, τ_{BE} with $\tau = \tau_{TT} \cup \tau_{M_i} \cup \tau_{BE}$ as the set of all the flows in the TSN network. The subscripts M_i ($i \in [1,7]$) for AVB denote respectively the different AVB traffic classes. For TT traffic, we know the GCL for TT traffic in each output port h of nodes, i.e., the opening and closing time of TT traffic (denoted with TT window) and GCL period (p^h_{GCL}). For an AVB flow $\tau_{M_i[k]} \in \tau_{M_i}$, we know its frame size $l_{M_i[k]}$, the minimum frame interval $p_{M_i[k]}$ in the source ES and the traffic class M_i it belongs to. The AVB Class M_i has higher priority than the AVB Class M_{i+1}. The flows assigned the same priority belong to the same AVB traffic class M_i, and frames within each traffic class are in FIFO order. Moreover, we know the maximum frame size l^{max}_{BE} of BE traffic.

III. TSN/GCL+CBS Output Port

The TSN Task group has defined a lot of mechanisms, which can interact in several ways. In this paper, we assume a specific configuration, calles TSN/GCL+CBS architecture and will present how TT and AVB flows are transmitted in this case. Fig. 2 gives an illustration for an output port of a node. Each one has eight queues for storing frames that wait to be forwarded on the corresponding link, one or more (N^h_{TT}) for TT queues, two or more (N^h_{CBS}) for AVB queues (respectively for Class M_i) and the remaining queues are used for BE. Every queue has a gate with two states, open and closed. Frames waiting in the queue are eligible to be forwarded only if the associated gate is open.

The gates for each queue are controlled by a GCL, which is created offline and contains the times when the associated

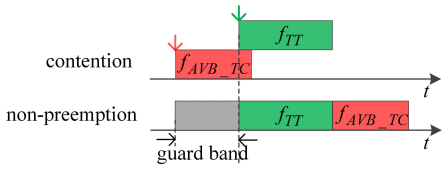

Fig. 3. Non-preemption integration modes

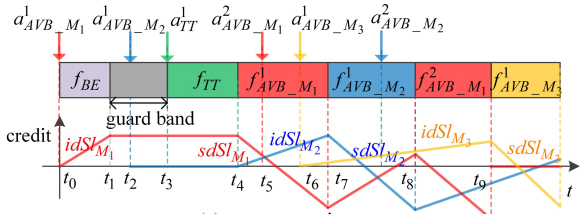

Fig. 4. CBS example with non-preemption mode

gates are open and closed [10], [25]. It is created such that when associated gate for TT traffic is open, the remaining gates for other traffic (AVB and BE) are closed, and vice versa (aka. exclusive gatig). Therefore, AVB traffic is prevented from transmitting in the time windows reserved for TT frames.

In addition, two integration modes are introduced to solve the issue when an AVB frame is already in transmission at the beginning of time window for TT, i.e., non-preemption and preemption modes. In this paper, we only focus on the discussion of the *non-preemption* integration mode (see Fig. 3) and preemption can be easily extended. The non-preemption mode uses a "guard band" before each TT window to prevent the AVB frame from initiating transmission if there is insufficient time available to transmit the entirely of that frame before the TT gate open. The non-preemption integration mode will lead to wasted bandwidth due to the guard band, but it ensures no delays for TT traffic.

An enqueued AVB frame is transmitted only if the associated gate is open and the Credit-Based Shaper (CBS) permits. Each AVB class has an associated credit value and is initialized to zero. When the associated AVB gate is open, the variation of credit is the same as the one in AVB network [7], i.e., decreasing with a send slope during the transmission of an AVB frame and increasing with an idle slope when AVB frames are waiting to be transmitted due to other higher priority AVB frames or the negative credit. When the AVB gate is closed, the associated credit is "frozen". This is illustrated for example in Fig. 4, where we have three classes of AVB traffic M_i ($i=1,2,3$), and show the variation of credit for respective AVB class. Particularly, during guard bands, we assume that the credit for AVB traffic is also "frozen", otherwise if increased may leading to a credit overflow problem thus causing the starvation of lower priority AVB traffic [26].

IV. Network Calculus Background

Network Calculus [27] is a mature theory proposed for deterministic performance analysis. It is used to construct arrival and service curve models for the investigated flows and network nodes. The arrival and service curves are defined by means of the min-plus convolution.

Network Calculus functions mainly belong to non-decreasing functions and null before 0: $\mathscr{F}_{\uparrow} = \{f : \mathbb{R}_+ \to \mathbb{R} | x_1 < x_2 \Rightarrow f(x_1) < f(x_2), x < 0 \Rightarrow f(x) = 0\}$. Two basic operators on $\mathscr{F}_{\uparrow}$ are the convolution $\otimes$,

$$(f \otimes g)(t) = \inf_{0 \le s \le t} \{f(t-s) + g(s)\}, \tag{1}$$

and deconvolution $\oslash$,

$$(f \oslash g)(t) = \sup_{s \ge 0} \{f(t+s) - g(s)\}, \tag{2}$$

where inf means infimum and sup means supremum.

An arrival curve $\alpha(t)$ is a model constraining the arrival process $R(t)$ of a flow, in which $R(t)$ represents the input cumulative function counting the total data bits of the flow that has arrived in the network node up to time t. We say that $R(t)$ is constrained by $\alpha(t)$ if

$$R(t) \le \inf_{0 \le s \le t} \{R(s) + \alpha(t-s)\} = (R \otimes \alpha)(t). \tag{3}$$

A service curve $\beta(t)$ models the processing capability of the available resource. Assume that $R^*(t)$ is the departure process, which is the output cumulative function that counts the total data bits of the flow departure from the network node up to time t. There are several definitions for service curve. We say that the network node offers the min-plus minimum service curve $\beta(t)$ for the flow

$$R^*(t) \ge \inf_{0 \le s \le t} \{R(s) + \beta(t-s)\} = (R \otimes \beta)(t), \tag{4}$$

and offers the strict service curve $\beta(t)$ iff

$$R^*(t+\Delta t) - R^*(t) \ge \beta(\Delta t), \tag{5}$$

during any backlog period $[t, t+\Delta t)$. In addition, in order to evaluate service curves we will use the non-decreasing non-negative closure defined by

$$[f(t)]^+_{\uparrow} = \max_{0 \le s \le t} \{f(s), 0\}.$$

If a flow $R(t)$ of arrival curve $\alpha(t)$ crosses a server with the service curve $\beta(t)$, then the output flow $R^*(t)$ can be bounded by the arrival curve $\alpha'(t)$,

$$\alpha'(t) = \alpha \oslash \beta(t) = \sup_{s \ge 0} \{\alpha(t+s) - \beta(s)\}, \tag{6}$$

It can also be taken as the arrival curve of input flow for the next node.

Let us assume that the flow constrained by the arrival curve $\alpha(t)$ traverses the network node offering the service curve $\beta(t)$. Then, the latency experienced by the flow in the network node is bounded by the maximum horizontal deviation between the graphs of two curves $\alpha(t)$ and $\beta(t)$,

$$h(\alpha, \beta) = \sup_{s \ge 0} \{\inf\{\tau \ge 0 \mid \alpha(s) \le \beta(s+\tau)\}\}. \tag{7}$$

With these definitions, the worst-case end-to-end delay of the flow is the sum of latency bounds in each network nodes along its routing.

V. Worst-case Analysis for AVB Traffic

A. Service Curve for AVB traffic with non-preemption mode

In this section, we will extend the service curve in [23] to multiple AVB Class M_i ($i \in [1, N^h_{CBS}]$) under non-preemption mode without considering any shaping curves.

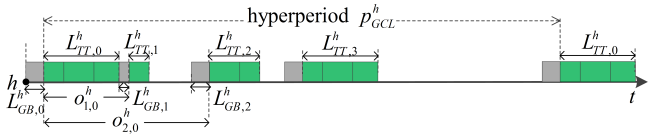

Fig. 5. Guard bands before TT windows

The service curve for AVB traffic depends on the remaining service from TT traffic which has the highest priority and is scheduled within specific TT windows according to GCLs. We assume that the GCL in an output port h has a set of periodic TT windows. Then, the GCL for the output port h is repeated after the GCL period p^h_{GCL}, which is the Least Common Multiple (LCM) of periods of all periodic TT windows in the output port h, see the example in Fig. 5. Thus, for a given GCL in an output port, we known the finite number (N^h_{TT}) of TT windows in the GCL period p^h_{GCL}. It is assumed that the time duration of the ith ($i \in [0, N^h-1]$) TT window in the output port h is $L^h_{TT,i}$, and the relative offset between the starting time of the ith and jth ($j \in [i+1, i+N^h-1]$) TT windows within the same GCL period is $o^h_{j,i}$ if taking the ith TT window as the reference. Note that $o^h_{j,i}$ equals to 0 if $j=i$. Moreover, with the consideration of the non-preemption mode, in the worst-case, the time duration of the guard band $L^h_{GB,i}$ before the ith ($i \in [0, N^h-1]$) TT window equals to the minimum value of the maximum transmission time of AVB frames competing in the output port h and the idle time interval between two consecutive TT windows, *i.e.*, $(i-1+N^h)\%N^h$th and ith windows. By merging the guard band effect into the construction of the TT aggregate arrival curve as discussed in [23], we have already known the following Lemma,

Lemma 1: The aggregate arrival curve for TT traffic and guard bands with the non-preemption mode in an output port h is given by

$$\alpha^h_{GB+TT}(t) = \max_{0\le i\le N^h-1}\{\alpha^h_{GB+TT,i}(t)\}$$
$$= \max_{0\le i\le N^h-1}\sum_{j=i}^{i+N^h-1}(L^h_{TT,j}+L^h_{GB,j})\cdot C\cdot\left\lceil\frac{t-o^h_{j,i}+L^h_{GB,j}-L^h_{GB,i}}{p^h_{\text{GCL}}}\right\rceil. \quad (8)$$

Moreover, the service curve for AVB traffic is also related to the CBS that supplied for each AVB Class M_i. Any time interval Δt can be decomposed by

$$\Delta t = \Delta t^+ + \Delta t^- + \Delta t^0, \quad (9)$$

where $\Delta t^+ = \sum_i \Delta t^+_i$ (resp. $\Delta t^- = \sum_j \Delta t^-_j$) represents the accumulated length of all period where the credit increases (resp. descreases), and $\Delta t^0 = \sum_k \Delta t^0_k$ is the frozen time of credit M_i due to the guard band and TT windows. For example in Fig. 6, there are two rising phases (Δt^+_1 and Δt^+_2), two descent phases (Δt^-_1 and Δt^-_2) and one frozen phase (Δt^0_1) of credit M_1. The service could only be supplied for AVB traffic during the descent time Δt^- of credit. Then, we extend the service curve for multiple classes of AVB traffic by the following theorem.

Theorem 1: The min-plus minimum service curve for AVB Class M_i ($i \in [1, N^h_{CBS}]$) with non-preemption mode in an output port h is given by

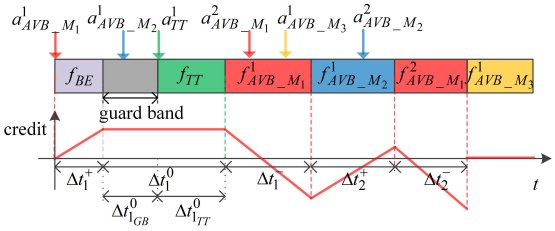

Fig. 6. Decomposed interval with non-preemption integration mode

port h is given by

$$\beta^{h[npr]}_{M_i}(t) = idSl_{M_i}\left[t - \frac{\alpha^h_{GB+TT}(t)}{C} - \frac{c^{max}_{M_i}}{idSl_{M_i}}\right]^+_{\uparrow}, \quad (10)$$

where $[npr]$ represents the non-preemption integration mode, $\alpha^h_{GB+TT}(t)$ is given by Lemma 1, and $c^{max}_{M_i}$ is the upper bound of credit M_i given by (12), which proof has to be extended to an arbitrary number of AVB classes and is one of challenges in this paper and will be discussed in Sect. V-B. The proof is similar as the one given to Theorem 1 in [23], hence will not be further discussed in this paper.

B. Bounding the credit for AVB traffic

In this section, we bound the credit for AVB traffic. Let us recall from Sect. III how AVB is transmitted. In TSN, the transmission of AVB traffic is not only related to the gate states, but also to CBS. Although TT transmission in non-preemption mode delays AVB traffic, the credits are frozen during these periods. Therefore, we can say that AVB credits will not be affected by TT traffic. In fact, the credit value is related to the transmission and backlog of AVB frames during the time when the respective AVB gates are open.

Theorem 2: (Lower bound of Class M_i) Let $l^{max}_{M_i}$ be the maximal frame size of any flow crossing the AVB queue Q_{M_i}. Then, the credit $c_{M_i}(t)$ of Class M_i is lower bounded by [12],

$$c^{min}_{M_i} = \frac{l^{max}_{M_i}}{C} sdSl_{M_i} \le c_{M_i}(t). \quad (11)$$

Proof: Since only when sending a frame of Class M_i the credit is decreased, the check of the lower bound must be done at the end of the emission of a frame of Class M_i. Considering the evolution of the credit, the minimal value of the credit is reached only when the size of the transmitted frame is the maximal one. In this situation the transmission period is defined as $\Delta t^{-max}_{M_i} = l^{max}_{M_i}/C$. Therefore, the credit at the end of the transmission is $c_{M_i}(t+\Delta t^{-max}_{M_i}) = 0 + sdSl_{M_i}\cdot l^{max}_{M_i}/C$. ■

Note that the constraint on $idSl_{M_i}$ and $sdSl_{M_i}$ for any AVB traffic class satisfies $sdSl_{M_i} = idSl_{M_i} - C$ [8].

Theorem 3: (Higher bound of Class M_i) Let l^{max}_{BE} be the maximal frame size of a BE flow. The credit $c_{M_i}(t)$ of Class M_i is upper bounded by,

$$c_{M_i}(t) \le \frac{l^{max}_{>i}}{C} idSl_{M_i} + \left(-\frac{l^{max}_{>i}}{C}\sum_{j=1}^{i-1} idSl_{M_j} + \sum_{j=1}^{i-1} c^{min}_{M_j}\right)\frac{idSl_{M_i}}{\sum_{j=1}^{i-1} idSl_{M_j} - C} = c^{max}_{M_i}, \quad (12)$$

where $l^{max}_{>i} = max_{j\in[i+1,N^h_{CBS}]}\{l^{max}_{M_j}, l^{max}_{BE}\}$ and $c^{min}_{M_j}$ is the lower bound of credit of Class M_j from Theorem 2.

Proof: Consider a time point t and the AVB queue Q_{M_i}. Let's note $Q^{\leq i}_{AVB} = \bigcup_{1\leq j\leq i}\{Q_{M_j}\}$ the same or higher priority AVB queues and $Q^{>i}_{AVB} = \bigcup_{i<j\leq N^h_{CBS}}\{Q_{M_j}\}$ the lower priority AVB queues.

If no frame is being sent at t, it means that for all $j \leq i$, $c_{M_j}(t) \leq 0$, otherwise a frame would be sent.

Now consider that a frame is being sent from $Q^{>i}_{AVB}$ or from the BE queue at t. Set s be the start of the emission of this frame. Notice that $t - s \leq l^{max}_{>i}/C$, where $l^{max}_{>i} = max_{j\in[i+1,N^h_{CBS}]}\{l^{max}_{M_j}, l^{max}_{BE}\}$. For all $j \leq i$, $c_{M_j}(t) \leq 0$, otherwise, at time s, an AVB frame from $Q^{\leq i}_{AVB}$ would have been selected for emission. Then we can deduce that for all $j \leq i$, $c_{M_j}(t) \leq idSl_{M_j} \cdot l^{max}_{>i}/C$.

Last consider that a frame is being sent from $Q^{\leq i}_{AVB}$ at t. Set x the last time before t where a frame from $Q^{\leq i}_{AVB}$ was not being sent. Let's denote Δt_{M_i} the duration of emissions of frames from queue Q_{M_i} between x and t. Then it is possible to upper bound the variation of credit of Class M_i between x and t,

$$\begin{aligned} c_{M_i}(t) - c_{M_i}(x) \leq & \Delta t_{M_i} \cdot sdSl_{M_i} + (t - x - \Delta t_{M_i}) \cdot idSl_{M_i} \\ = & -\Delta t_{M_i} \cdot C + (t-x) \cdot idSl_{M_i}. \end{aligned} \tag{13}$$

Let $c_{<i}(t) = \sum_{j=1}^{i-1} c_{M_j}(t)$ denote the sum of credits of AVB traffic with the priority higher than M_i. Then at any instant between x and t either a frame from Class M_i is being sent, in this case $c_{<i}(t)$ increase at most at speed $\sum_{j=1}^{i-1} idSl_{M_j}$. Either a frame from class with higher priority than M_i is being sent, in this case $c_{<i}(t)$ decrease at least at speed $\sum_{j=1}^{i-1} idSl_{M_j} - C$ (all the classes from $Q^{<i}_{AVB}$ gain credit expect one which loses credit). Then it is possible to upper bound the variation of $c_{<i}(t)$ between x and t,

$$\begin{aligned} & c_{<i}(t) - c_{<i}(x) \\ & \leq \Delta t_{M_i} \cdot \sum_{j=1}^{i-1} idSl_{M_j} + (t - x - \Delta t_{M_i}) \cdot \left(\sum_{j=1}^{i-1} idSl_{M_j} - C \right) \\ & = \Delta t_{M_i} \cdot C + (t-x) \cdot \left(\sum_{j=1}^{i-1} idSl_{M_j} - C \right). \end{aligned}$$

Since $\sum_{j=1}^{i-1} idSl_{M_j} - C < 0$, then we have

$$t - x \leq \frac{c_{<i}(t) - c_{<i}(x) - \Delta t_{M_i} \cdot C}{\sum_{j=1}^{i-1} idSl_{M_j} - C}. \tag{14}$$

Then from (14), (13) is modified to obtain,

$$c_{M_i}(t) - c_{M_i}(x) \leq (c_{<i}(t) - c_{<i}(x)) \frac{idSl_{M_i}}{\sum_{j=1}^{i-1} idSl_{M_j} - C} - \Delta t_{M_i} C$$

$$\cdot \left(\frac{\sum_{j=1}^{i} idSl_{M_j} - C}{\sum_{j=1}^{i-1} idSl_{M_j} - C} \right) \leq (c_{<i}(t) - c_{<i}(x)) \frac{idSl_{M_i}}{\sum_{j=1}^{i-1} idSl_{M_j} - C}.$$

We have already proved that for all $j \leq i$, $c_{M_j}(x) \leq idSl_{M_j} \cdot l^{max}_{>i}/C$, therefore $c_{<i}(x) \leq \sum_{j=1}^{i-1} idSl_{M_j} \cdot l^{max}_{>i}/C$. Moreover if $c^{min}_{M_j}$ is the lower bound of credit of Class M_j, then $c_{<i}(t) \geq \sum_{j=1}^{i-1} c^{min}_{M_j}$ so to conclude,

$$\begin{aligned} c_{M_i}(t) \leq & \frac{l^{max}_{>i}}{C} idSl_{M_i} + \\ & \left(- \frac{l^{max}_{>i}}{C} \sum_{j=1}^{i-1} idSl_{M_j} + \sum_{j=1}^{i-1} c^{min}_{M_j} \right) \frac{idSl_{M_i}}{\sum_{j=1}^{i-1} idSl_{M_j} - C}. \end{aligned}$$

■

C. Tighter latency bounds by introducing shaping curves for arrival of AVB traffic

According to Network Calculus, the upper bound latency of a Class M_i flow $\tau_{M_i[k]}$ in the output port h is given by the maximum horizontal deviation between the aggregate arrival curve $\alpha^h_{M_i}(t)$ of intersecting flows of AVB Class M_i and the service curve $\beta^{h[npr]}_{M_i}(t)$ for AVB Class M_i in h,

$$D^h_{M_i[k]} = h(\alpha^h_{M_i}(t), \beta^{h[npr]}_{M_i}(t)), \tag{15}$$

where the service curve $\beta^{h[npr]}_{M_i}(t)$ is from Theorem 1.

In this paper, we provide a solution that leads to tighter aggregate arrival curves for AVB traffic in intermediate nodes, reducing thus the pessimism of WCDs for AVB flows by considering the shaping caused by the physical link speed and the CBS.

The individual arrival curve for the flow $\tau_{M_i[k]}$ in the source ES (h_0) can be given by

$$\alpha^{h_0}_{M_i[k]}(t) = l_{M_i[k]} + \frac{l_{M_i[k]}}{p_{M_i[k]}} \cdot t \tag{16}$$

where $l_{M_i[k]}$ is the burst of the flow in h_0, $l_{M_i[k]}/p_{M_i[k]}$ is the long-term rate of $\tau_{M_i[k]}$ sending from the source ES.

The individual arrival curve $\alpha^h_{M_i[k]}$ for the flow $\tau_{M_i[k]}$ in the output port h of intermediate nodes is calculated from the previous node port h' along the path of $\tau_{M_i[k]}$. Moreover, flows $\tau_{M_i[k]}$ of Class M_i waiting in the queue of h and from the same previous node port h' are taken as a group, as they cannot simultaneously arrive because of sharing a physical link, and will be limited by the CBS. We assume that $\alpha^h_{M_i,h'}(t)$ represents the grouping arrival curve from the same node port h' and is given by,

$$\begin{aligned} \alpha^h_{M_i,h'}(t) = & \Big(\sum_{\tau_{M_i[k]}\in[h',h]} \alpha^{h'}_{M_i[k]}(t) \oslash \delta^{h'}_{D_i}(t) \Big) \\ & \wedge (\sigma^{h'}_{M_i}(t) + l^{h,max}_{M_i,h'}) \wedge (\sigma_{link}(t) + l^{h,max}_{M_i,h'}), \end{aligned} \tag{17}$$

where $\alpha^{h'}_{M_i[k]}(t) \oslash \delta^{h'}_{D_{M_i}}(t)$ is the output arrival curve considering the queuing delay, $\delta_D(t)$ is the burst-delay function which equals to 0 if $t \leq D$ and ∞ otherwise, $x \wedge y = min\{x, y\}$, $\sigma_{link}(t) = C \cdot t$ is the shaping curve of physical link, $l^{h,max}_{M_i,h'}$ is the maximum frame size of flows of Class M_i from h' to h, and $\sigma^{h'}_{M_i}(t)$ is the shaping curve of CBS, which will be discussed in Sect. V-D with the consideration of TT effects.

Then the aggregate arrival curve $\alpha^h_{M_i}(t)$ for the output port h is the sum of all grouping arrival curves of Class M_i. Moreover, it is assumed of no limitation for arriving of flows in the source ES (h_0). Then they can simultaneously arrive and thus the aggregate arrival curve $\alpha^{h_0}_{M_i}(t)$ for the port h_0 is the sum of all individual arrival curves of Class M_i flows.

By disseminating the computation of latency bounds along

the routing of $\tau_{M_i[k]}$, its WCD is obtained by the sum of delays from its source ES to its destination ES,

$$D_{M_i[k]} = \sum_{h \in dr_{M_i[k]}} D^h_{M_i[k]} + (h-1) \cdot d_{tech}, \tag{18}$$

where d_{tech} is the constant technical latency in a SW.

D. CBS Shaping Curve for AVB traffic

Shaping curve is a concept which characterizes the maximum number of bits that are served during a period of time Δt. A server offers a shaping curve $\sigma(t)$ iff $\sigma(t)$ could be an arrival curve for all output cumulative function $R^*(t)$, i.e.,

$$R^*(t+\Delta t) - R^*(t) \leq \sigma(\Delta t), \tag{19}$$

where $R^*(t)$ is the output cumulative function.

Lemma 2: With the non-preemption mode, the strict service curve for TT traffic in an output port h is given by,

$$\beta^h_{TT}(t) = min_{0 \leq i \leq N^h-1} \left\{ \sum_{j=i}^{i+N^h-1} \beta^h_{TDMA}(t+t_0, L_{TT,j}) \right\}, \tag{20}$$

where

$$\beta^h_{TDMA}(t, L_{TT}) = C \cdot max\left\{ \left\lfloor \frac{t}{p^h_{\mathrm{GCL}}} \right\rfloor L^h_{TT}, t - \left\lceil \frac{t}{p^h_{\mathrm{GCL}}} \right\rceil (p^h_{\mathrm{GCL}} - L^h_{TT}) \right\},$$

and

$$t_0 = p^h_{\mathrm{GCL}} - L^h_{TT_j} - o^h_{0,i} - o^h_{j,i}.$$

Proof: As discussed in Sect. V-A, for a given GCL in an output port, there are N^h number of TT windows in the GCL period p^h_{GCL}. Then the service for TT traffic can be taken as N^h sets of periodic windows with the known length and relative offsets.

If considering one set of periodic (p^h_{GCL}) TT windows of length L_{TT}, its service in the port h is similar to the TDMA communication [28]. In the worst-case time interval $p^h_{\mathrm{GCL}} - L^h_{TT}$ is not supplied for the TT traffic, and has exclusive service of the bandwidth for TT during the interval L^h_{TT} afterwards. Therefore, the service cannot be guaranteed during any time interval $0 \leq \Delta t < p^h_{\mathrm{GCL}} - L^h_{TT}$, but can be guaranteed of $C \cdot (\Delta t - p^h_{\mathrm{GCL}} - L^h_{TT})$ in any time interval $p^h_{\mathrm{GCL}} - L^h_{TT} \leq \Delta t < p^h_{\mathrm{GCL}}$. Then the service curve supplied for the set of periodic TT windows during Δt can be given by,

$$\beta^h_{TDMA}(\Delta t, L_{TT}) = C \cdot max\left\{ \left\lfloor \frac{\Delta t}{p^h_{\mathrm{GCL}}} \right\rfloor L^h_{TT}, \Delta t - \left\lceil \frac{\Delta t}{p^h_{\mathrm{GCL}}} \right\rceil (p^h_{\mathrm{GCL}} - L^h_{TT}) \right\}. \tag{21}$$

Then the service for all N^h sets of periodic TT windows is derived from (21) as well as the relative offsets between two TT windows from different sets. Taking the ith ($i \in [0, N^h-1]$) TT window as the reference, we have that the first served frame is from the ith TT window during the backlogged period Δt. Assume that $o^h_{0,i}$ is the maximum idle time interval before the opening time of the ith window, then the service guaranteed for the ith set of TT windows is the curve in (21) shifted to the left with the positive value $p^h_{\mathrm{GCL}} - L^h_{TT,i} - o^h_{0,i}$,

$$\beta^h_{TT,i,i}(\Delta t) = \beta^h_{TDMA}(\Delta t + p^h_{\mathrm{GCL}} - L^h_{TT,i} - o^h_{0,i}, L_{TT,i}).$$

Moreover, for the other set of the jth ($j \in [i+1, i+N^h-1]$) traffic windows, with the known of the relative offset $o^h_{j,i}$ by considering the ith TT window as the benchmark, the service guaranteed for TT traffic in the jth set of windows can be given by shifting the curve in (21) to the left with the positive value $p^h_{\mathrm{GCL}} - L^h_{TT,j} - o^h_{0,i} - o^h_{j,i}$,

$$\beta^h_{TT,j,i}(\Delta t) = \beta^h_{TDMA}(\Delta t + p^h_{\mathrm{GCL}} - L^h_{TT,j} - o^h_{0,i} - o^h_{j,i}, L_{TT,j}).$$

Note that $\beta^h_{TT,j,i}(\Delta t)$ equals to $\beta^h_{TT,i,i}(\Delta t)$ if $j = i$.

Thus if the ith TT window as benchmark, the strict service for TT traffic is as follows after considering all N^h sets of periodic TT windows,

$$\beta^h_{TT,i}(\Delta t) = \sum_{j=i}^{i+N^h-1} \beta^h_{TT,j,i}(\Delta t).$$

Then the strict service curve for TT traffic in an output port h is the lower envelope of $\beta^h_{TT,i}(\Delta t)$ by considering each TT windows in the GCL period as benchmark,

$$\beta^h_{TT}(\Delta t) = min_{0 \leq i \leq N^h-1}\{\beta^h_{TT,i}(\Delta t)\}.$$

■

Theorem 4: The CBS shaping curve of Class M_i for the non-preemption mode is given by,

$$\sigma^h_{M_i}(t) = \left[t - \frac{\beta^h_{TT}(t)}{C} \right]^+_{\uparrow} \cdot idSl_{M_i} + c^{max}_{M_i} - c^{min}_{M_i}, \tag{22}$$

where $\beta^h_{TT}(t)$ is given by the Lemma 2, and $c^{max}_{M_i}$ and $c^{min}_{M_i}$ are respectively the upper and lower bounds of credit of M_i given by (12) and (11).

Proof: For an arbitrary period of time Δt, the variation of credit during Δt satisfies

$$\begin{aligned} \Delta c_{M_i} &= c_{M_i}(t+\Delta t) - c_{M_i}(t) = \Delta t^+ \cdot idSl_{M_i} + \Delta t^- \cdot sdSl_{M_i} \\ &= (\Delta t - \Delta t^0) \cdot idSl_{M_i} - \Delta t^- \cdot (idSl_{M_i} - sdSl_{M_i}). \end{aligned} \tag{23}$$

In the best-case, the frozen duration is only related to TT windows, and has nothing to do with guard bands, for the non-preemption integration mode. Considering the strict service curve of TT traffic expressed in the Lemma 2, Δt^0 is limited by,

$$R^{h*}_{TT}(t+\Delta t) - R^{h*}_{TT}(t) = \Delta t^0 \cdot C \geq \beta^h_{TT}(\Delta t). \tag{24}$$

Moreover, Δt^- can be expressed by,

$$R^{h*}_{M_i}(t+\Delta t) - R^{h*}_{M_i}(t) = \Delta t^- \cdot C, \tag{25}$$

and Δc_{M_i} satisfies the relationship as follows,

$$\Delta c_{M_i} \geq c^{min}_{M_i} - c^{max}_{M_i}. \tag{26}$$

Due to non-decreasing function $R^{h*}_{M_i}(t)$ and using the expressions (24), (25), (26) and $sdSl_{M_i} = idSl_{M_i} - C$, (23) is modified to obtain,

$$R^{h*}_{M_i}(t+\Delta t) - R^{h*}_{M_i}(t) \leq \left[\Delta t - \frac{\beta^h_{TT}(\Delta t)}{C} \right]^+_{\uparrow} \cdot idSl_{M_i} + c^{max}_{M_i} - c^{min}_{M_i}.$$

Considering the definition of the shaping curve in (19), the CBS shaping curve of AVB traffic of Class M_i is given by,

$$\sigma^h_{M_i}(t) = \left[t - \beta^h_{TT}(t)/C \right]^+_{\uparrow} \cdot idSl_{M_i} + c^{max}_{M_i} - c^{min}_{M_i}.$$

■

VI. Experimental Results

We have evaluated our proposed improving Network Calculus-based WCD analysis for multiple AVB classes in TSN (called PL/CBS-NC/TSN) as follows. PL/CBS-NC/TSN is implemented in C++ using the Java kernel of the RTC toolbox [29], running on a computer with Intel Core i7-3520M CPU at 2.90 GHz and 4 GB of RAM.

A. Synthetic Test Cases

In this section, our evaluation focuses on a tree topology of 6 ESes and 2 SWs, connected via physical links with rates of 100Mb/s, as shown in Fig. 7.

Firstly, we are interested to show the improvement of AVB WCDs in TSN network obtained with our proposed method by considering physical link and CBS shaping curves in comparison to existing work [23]. The test case (TC1) has 5 TT flows and 10 AVB flows of only two classes (M_1 and M_2), as in order to compare with the model proposed in [23]. The physical link rate is 100Mb/s, the average load of links is about 14.2% and the maximum link load is about 33.1%. The idle slopes of Class M_1 and Class M_2 are respectively set to 40% and 20% [(2)].

The WCDs for each AVB flow of TC1 are calculated under different timing analysis models. The results of the comparison between [23] (NC/TSN) and the proposed method (PL/CBS-NC/TSN) are presented in Table I. As we can see, our method by introducing physical link shaping and CBS shaping curves is able to significantly reduce the WCDs compared to [23], with 17.0% on average and 26.4% in maximum. Moreover, we also present the results obtained with our method, where we have only used physical link shaping but we have not used CBS shaping curves, denoted with PL-NC/TSN. As we can see from the third column in Table I, PL-NC/TSN is able to reduce on average the WCDs obtained with [23] by 5.6% and as much as 9.7% in some cases. Additionally, we give simulation results in the last column. The simulation results denoted with Sim are useful for validating our approach, as our obtained WCDs should all be larger than the maximum delays obtained by simulation, which is the case in our experiments. However, as rare events can be missed, a simulation approach will not be able to determine the WCDs, hence it is not useful for safety critical applications that require safety guarantees.

In the second experiment, we would like to evaluate the scalability of our analysis PL/CBS-NC/TSN with the number of TT flows and to show the correctness of our analysis by comparing with simulation results. We use another test case (TC2) by extending TC1 such that it has a total of 50 TT flows. The obtained results are visually shown in Fig. 8, where on the x-axis we have the AVB flows, from AVB1 to AVB12, and on the y-axis we have the WCD values. As shown in Fig. 8, the obtained results are grouped by the AVB Classes with vertical dotted lines and respectively sorted in increasing order by results from TC1. TC1 is depicted with a red triangle and TC2 with a blue cross. As expected, the WCDs of the AVB flows grow with the increasing number of TT flows shown in Fig. 8. In addition, the average WCD (horizontal dotted lines) of Class M_1 is smaller than M_2, since the AVB class of higher priority has larger bandwidth guarantee, *i.e.*, $idSl_{M_1} > idSl_{M_2}$.

[(2)]More detailed information, including GCL for TT flows routes for each flow etc. can be downloaded from https://zenodo.org/record/2439362#.XBsMS84zbDc.

TABLE I
Compared results with and without shaping curve

Flow	NC/TSN [23] (μs)	PL-NC/TSN (μs)	PL/CBS-NC/TSN (μs)	Sim (μs)
AVB1	5378	5218	4470	2454
AVB2	4692	4640	4349	2594
AVB3	7128	6775	4851	2812
AVB4	3557	3224	2594	1401
AVB5	7083	6730	4806	2016
AVB6	3780	3392	2651	1508
AVB7	7211	6858	4934	2550
AVB8	2505	2357	2019	1097
AVB9	3557	3224	2594	1398
AVB10	3780	3392	2651	1401
AVB11	3178	2790	2049	1067
AVB12	7211	6858	4934	2248

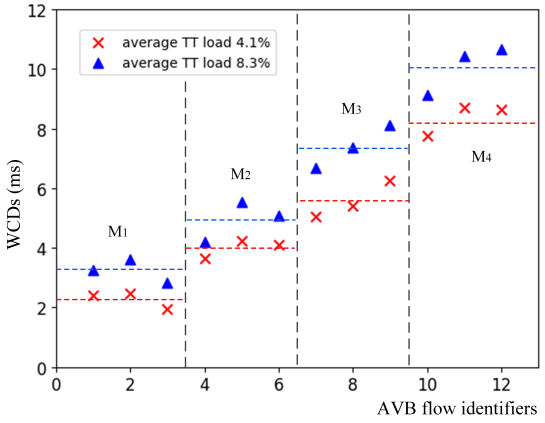

Fig. 8. WCDs for an increasing number of TT flows: from 5 to 50; AVB flows have been reordered based on their WCDs within each traffic class

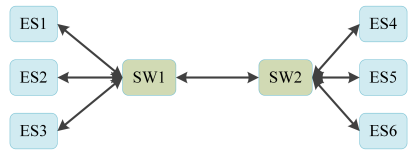

Fig. 7. The topology of synthetic small test cases

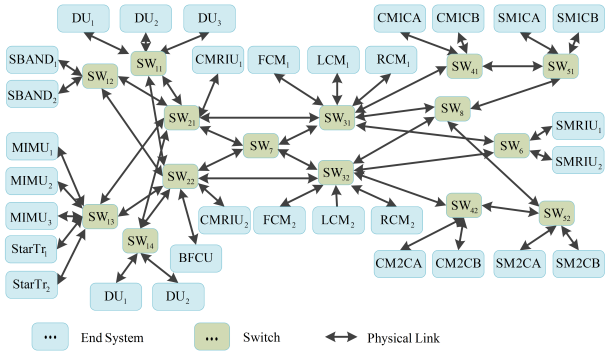

Fig. 9. Network topology of the Orion CEV

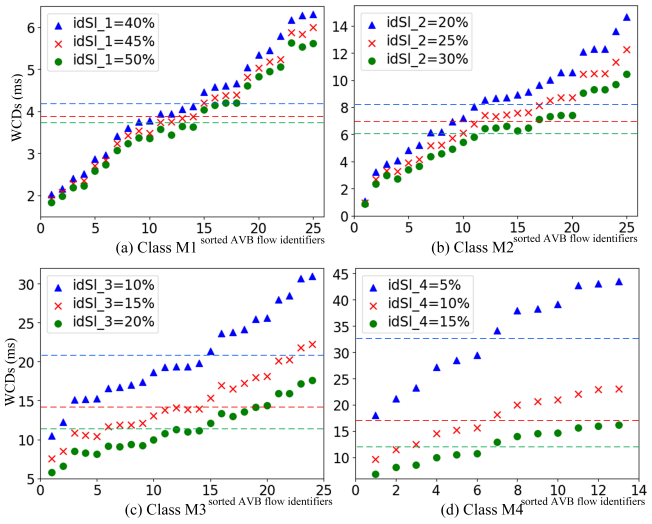

Fig. 10. WCDs decrease with increasing idle slopes

B. Evaluation on a Larger Realistic Test Case

For the final experiment, we use a larger real-world test case (TC3), adapted from the Orion Crew Exploration Vehicle (TC3) [30] by using the same topologies and TT flows, and considering rate-constrained (RC) flows as AVB flows. We investigate the scalability of our method and the influence of varied idle slopes on multiple classes of AVB traffic. CEV has a topology consisting of 31 ESes, 15 SWs, 188 dataflow routes, as shown in Fig. 9, connected by dataflow links transmitting at 1 Gbps, and running 100 TT flows, 25 AVB flows of Class M_1, 25 AVB flows of Class M_2, 24 AVB flows of Class M_3 and 13 AVB flows of Class M_4 (including multicast flows).

The expectation is that higher values for the idle slope will allow the AVB flows to pass faster through switches, reducing their WCDs. For AVB traffic, the idle slope $idSl_{M_i}$ is commonly established for granting just enough credit required to preserve the accumulated rate of all AVB Class M_i flows. In this experiment, the reference of idle slopes of M_1, M_2, M_3 and M_4 are respectively 40%, 20%, 10% and 5%. Then we increase the $idSl_{M_i}$ by keeping $idSl_{M_j}$ $(j \neq i)$ of other AVB class unchanged. The WCDs obtained by considering varying idle slopes for each AVB traffic Class are shown respectively in Fig. 10(a), (b), (c) and (d). Moreover, the results are sorted in increasing order and the average WCD under each case of idle slope is given by the horizontal dotted lines. As expected, the latency for AVB traffic declines with the increasing idle slopes, since the larger the idle slope, the higher the bandwidth guarantee is. For example, $idSl_{M_1}$ increasing from 40% to 45% leads to a decrease of WCD of AVB Class M_1 traffic with 5.6% on average.

VII. Conclusion

The TSN IEEE task group is defining new extensions of Ethernet, devoted to real-time and safety-critical application areas. These types of applications require a method to bound the worst-case delays of a given configuration. This paper has presented an improved Network Calculus-based approach by considering the limitations from physical link rate and the output of CBS, which are modeled as shaping curves to compute tighter bounds. Moreover, the timing analysis method has be extended to arbitrary number of AVB traffic classes in the case of a TSN/GCL+CBS architecture, *i.e.*, a system where one or more queues are scheduled in a Time-Triggered way, with exclusive access to the output link (excluding gating), and the others are shaped by a CBS credit (like in AVB).

Our analysis is, to the best of our knowledge, the first one to handle with any number of AVB classes. We have evaluated the proposed approach on both synthetic and realistic test cases. The experimental results and the comparison to the existing approaches show that the Network Calculus approach is a viable approach for the analysis of TSN. Our approach provides safe upper bounds on WCDs, reduces the pessimism of the analysis (tighter WCD bounds), and is scalable to handle large problem sizes.

References

[1] IEEE, "802.3 Standard for Ethernet," 2015.
[2] J. D. Decotignie, "Ethernet-based real-time and industrial communications," *Proceedings of the IEEE*, vol. 93, no. 6, pp. 1102-1117, 2005.
[3] ARINC 664, Aircraft Data Network, Part 7: Deterministic networks, 2003.
[4] SAE AS6802: Time-Triggered Ethernet, Technical report, 2011.
[5] D. Jansen, and B. Holger, "Real-time Ethernet: the EtherCAT solution," *Computing and Control Engineering*, vol. 15, no. 1, pp. 16-21, 2004.
[6] IEEE, "Time-Sensitive Networking Task Group," http://www.ieee802.org/1/pages/tsn.html, 2016.
[7] IEEE, "802.1BA—Audio Video Bridging (AVB) Systems," http://www.ieee802.org/1/pages/802.1ba.html, 2011.
[8] IEEE, "802.1Qbv—Enhancements for Scheduled Traffic," http://www.ieee802.org/1/pages/802.1bv.html, 2015.
[9] IEEE, "802.1ASrev—Timing and Synchronization for Time-Sensitive Applications," http://www.ieee802.org/1/pages/802.1AS-rev.html, 2017.
[10] S. S. Craciunas, R. Serna Oliver, M. Chmelik, and W. Steiner, "Scheduling Real-Time Communication in IEEE 802.1Qbv Time Sensitive Networks," in *Proc. of the 24th Int. Conf. on Real-Time Networks and Systems*, 2016.
[11] R. Queck, "Analysis of Ethernet AVB for automotive networks using network calculus," in *Proc. of IEEE Int. Conf. on Vehicular Electronics and Safety*, 2012.
[12] J. A. R. Azua, and M. Boyer, "Complete modelling of AVB in network calculus framework," in *Proc. of the 22nd Int. Conf. on Real-Time Networks and Systems*, 2014.
[13] A. Philip, D. Thiele, R. Ernst, and J. Diemer, "Exploiting shaper context to improve performance bounds of ethernet avb networks," in *Proc. of the 51st Annual Design Automation Conference*, 2014.
[14] J. Y. Cao, P. J. L. Cuijpers, R. J. Bril, and J. J. Lukkien, "Tight worst-case response-time analysis for ethernet AVB using eligible intervals," in *Proc. of the World Conf. on Factory Communication Systems*, 2016.
[15] L. Zhao, F. He, and E. Li, "Improving worst-case delay analysis for traffic of additional stream reservation class in Ethernet-AVB Network," *Sensors*, vol 18, no. 11, 2018.
[16] L. X. Zhao, H. G. Xiong, Z. Zheng, and Q. Li, "Improving worst-case latency analysis for rate-constrained traffic in the time-triggered ethernet network." *IEEE Communications Letters*, vol. 18, no. 11, pp. 1927-1930, 2014.
[17] M. Boyer, H. Daigmorte, N. Navet, and J. Migge, "Performance impact of the interactions between time-triggered and rate-constrained transmissions in TTEthernet," http://orbilu.uni.lu/handle/10993/23845, 2016.
[18] L. X. Zhao, P. Pop, Q. Li, J. Y. Chen, and H. G. Xiong, "Timing analysis of rate-constrained traffic in TTEthernet using network calculus," *Real-Time Systems*, vol. 53, no. 2, pp. 254-287, 2017.
[19] D. Thiele, R. Ernst, J. Diemer "Formal Worst-Case Timing Analysis of Ethernet TSN's Time-Aware and Peristaltic Shapers," in *Proc. of the IEEE Vehicular Networking Conference*, 2015.
[20] E. Mohammadpour, E. Stai, M. Mohiuddin, and J.-Y. Le Boudec, "End-to-end Latency and Backlog Bounds in Time-Sensitive Networking with Credit Based Shapers and Asynchronous Traffic Shaping," arXiv:1804.10608, 2018.

[21] D. Maxim, and Y. Q. Song, "Delay Analysis of AVB traffic in Time-Sensitive Networks (TSN)," in *Proc. of the 25th Int. Conf. on Real-Time Networks and Systems*, 2017.

[22] S. M. Laursen, P. Pop, and W. Steiner, "Routing Optimization of AVB Streams in TSN Networks," *ACM Sigbed Review*, vol. 13, no. 4, pp. 43-48, 2016.

[23] L. X. Zhao, P. Pop, Z. Zheng, and Q. Li, "Timing Analysis of AVB Traffic in TSN Networks using Network Calculus," in *Proc. of 24th Real Time and Embedded Technology and Applications Symposium*, 2018.

[24] IEEE, "802.1Q—Local and Metropolitan Area Networks-Bridges and Bridged Networks", 2018.

[25] P. Pop, M. L. Raagaard, S. S. Craciunas, and W. Steiner, "Design optimisation of cyber-physical distributed systems using IEEE time-sensitive networks," *IET Cyber-Physical Systems: Theory & Applications*, vol. 1, no. 1, pp.86-94, 2016.

[26] H. Daigmorte, and M. Boyer, "Does the integration of CBS and GCL behaves as you expect? And can it be enhanced?", 2018. ¡hal-01961718¿

[27] J. Y. Le Boudec, and P. Thiran, "Network calculus: A theory of deterministic queuing systems for the internet," *Springer-Verlag Lecture Notes on Computer Science*, 5th ed., New York, 2001.

[28] W. Ernesto, L. Thiele, "Optimal TDMA time slot and cycle length allocation for hard real-time systems," *Proc. of the 2006 Asia and South Pacific Design Automation Conference*, 2006.

[29] E. Wanderler, and L. Thiele, "Real-Time Calculus (RTC) Toolbox," http://www.mpa.ethz.ch/Rtctoolbox, 2006.

[30] D. Tamas-Selicean, P. Pop, and W. Steiner, "Design optimization of TTEthernet-based distributed real-time systems," *Real-Time Systems*, vol. 51, no. 1, pp.1-35, 2015.